




Large deformations of Timoshenko and Euler beams under distributed load

A. Della Corte , A. Battista, F. dell'Isola and P. Seppecher

Abstract. In this paper, the general equilibrium equations for a geometrically nonlinear version of the Timoshenko beam are derived from the energy functional. The particular case in which the shear and extensional stiffnesses are infinite, which correspond to the inextensible Euler beam model, is studied under a uniformly distributed load. All the global and local minimizers of the variational problem are characterized, and the relative monotonicity and regularity properties are established.

Mathematics Subject Classification. 74B20, 34B15, 49J45.

Keywords. Nonlinear elasticity, Timoshenko beam, Euler beam, Stability of solutions of nonlinear ODEs.

1. Introduction

Since the first mathematically consistent theory of *Elastica*, by Leonhard Euler and Bernoulli brothers (see [1–3]), a great deal of effort has been devoted to the study of beam models, due to their theoretical relevance as a 1D elastic model as well as their importance in structural engineering both as a static and a dynamic element. A rich literature exists considering both linearized and geometrically nonlinear models [4–9] together with generalized 1D elastic models (see [10, 11]), among which beam models capable to take into account other deformations than deflection, extension and shear (see for instance [12–16]). However, two aspects in geometrically nonlinear beam theory especially require further investigation: the behavior of the system under a distributed load and the related multiplicity of arising solutions. An analysis in these directions has been started in the work [17], where an inextensible Euler beam has been considered. In the present work, we extend the results presented in [18], introducing a geometrically nonlinear generalization of an extensible Timoshenko beam under a distributed load and characterizing all the stable equilibrium configurations of the inextensible *Elastica*.

The necessity of considering distributed loads in large deformation arises, for instance, in the field of fluid-structure interaction [19–23] or in the framework of microstructured continua [24, 25], in particular when the microstructure can be modeled as an array of fibers that can be individually modeled as beams undergoing large deformations, while the interaction with the remaining part of the array can be modeled as a distributed load acting on the beam. Possible examples are the structures described in [18, 26–33], which contributed to motivate the present study. The importance of fibrous microstructured systems is increasing in current literature, especially since these objects can be manufactured with great precision and relatively limited costs by means of computer-aided manufacturing (see for instance [34, 35] for useful reference works). Therefore, investigating the behavior of their elementary constituents in geometrically nonlinear deformation is more relevant nowadays. Moreover, equations similar to those describing the equilibrium of beams can also be found in different contexts: That is the case for instance when describing the separation line of self-adhesive polymeric films [36].

Surprisingly, enough there are not many results in the literature, in particular, rigorous ones, concerning nonlinear deformation of beams under distributed load. The classical reference work [4] only covers

the case of concentrated load. Afterward, some numerical results for the inextensible Euler beam under distributed load were published in [37, 38].

The paper is organized as follows: in Sect. 2 a nonlinear version of the extensible Timoshenko beam model is introduced and the problem of a clamped-free beam is formulated. Euler–Lagrange equations are formally derived. In Sect. 3, some numerical results concerning curled equilibrium configurations are shown. These results motivate the analytical study of the properties of the equilibrium solutions done in Sect. 4, in which the Euler–Lagrange equation is studied in the particular case of an infinite shear stiffness, which leads to the nonlinear Euler beam.

2. The model

In this section, we introduce a general Timoshenko model and formally derive the Euler–Lagrange equations associated with the minimization of the total energy.

2.1. Kinematics and deformation energy

We consider a beam lying in a two-dimensional space E in which we fix once and for all an orthonormal reference system $\{\mathbf{e}_1, \mathbf{e}_2\}$. The beam can be understood as the section of a plate which is in planar strain or stress state. The placement of the beam is described by a pair $(\boldsymbol{\chi}, \varphi)$ of functions defined on the interval $[0, L]$ and taking values, respectively, in E and \mathbb{R} : $\boldsymbol{\chi}(s)$ represents the position of a point s of the beam while φ is an extra kinematic variable attached to point s . In the classical presentation of Timoshenko linear model in the early 1920s (see [39, 40]), φ is thought to represent the angle of rotation of the sections of the beam (supposed rigid) with respect to the normal to the neutral axis. It is well known that this standard Timoshenko beam model is a particular case of a linear Cosserat 1D continuum in which φ is thought to represent an internal rotational degree of freedom (the original work by Cosserat brothers is [41]; see for instance [42, 42, 43] for interesting applications). The chosen mechanical interpretation of φ is in fact irrelevant. Anyway, we classically call “couple” the dual variable to φ while we call “force” the dual variable to $\boldsymbol{\chi}$.

We assume that, at rest, the beam lies along \mathbf{e}_1 so that its placement $(\boldsymbol{\chi}_0, \varphi_0)$ is given $\forall s \in [0, L]$ by $\boldsymbol{\chi}_0(s) = s\mathbf{e}_1$ and $\varphi_0(s) = 0$ so that L stands for the length of the beam at rest. The beam is clamped at the extremity point $s = 0$ (in the sense that $\boldsymbol{\chi}(0) = 0$ and $\varphi(0) = 0$) and this point coincides with the origin of the reference axes.

We introduce the tangent vector to the actual configuration and write it under the form

$$\boldsymbol{\chi}'(s) = \alpha(s)\mathbf{e}(\theta(s)) \quad (1)$$

where

$$\alpha := \|\boldsymbol{\chi}'\| \geq 0, \quad \text{and} \quad \mathbf{e}(\theta) := \cos(\theta)\mathbf{e}_1 + \sin(\theta)\mathbf{e}_2$$

The quantity α accounts for the elongation of the beam, while $\theta(s)$ is the angle that $\boldsymbol{\chi}'(s)$ forms with \mathbf{e}_1 .

As at rest $\alpha = 1$ and $\varphi = \theta = 0$, we assume that the deformation of the beam can be measured by the quantities $\alpha - 1$, φ' and $\varphi - \theta$ and that the associated energy reads

$$\int_0^L \left\{ k_e f(\alpha(s)) + \frac{k_b}{2} (\varphi'(s))^2 + \frac{k_t}{2} (\varphi(s) - \theta(s))^2 \right\} ds \quad (2)$$

where f is a C^1 function on $]0, +\infty[$ which is: i) positive; ii) convex; iii) tending to $+\infty$ when x tends to 0 or $+\infty$. We extend it on \mathbb{R} by setting $f(x) = +\infty$ when $x \leq 0$ (in the numerical section we will use the function $f(\alpha) = -0.01 \log(\alpha) + (\alpha - 1)^2$ for $x > 0$); as it is easily seen, this function has the desired

properties and is very close to $(\alpha - 1)^2$ except in the vicinity of the origin, where it diverges rapidly). We also introduce the derivative g of f on $]0, +\infty[$.

The three addends in the previous integral are, respectively, called “extensional energy,” “flexural energy” and “shear energy” and the positive material parameters k_e , k_b and k_t are the associated stiffnesses.

It is well known that, in the classical Timoshenko formulations in terms of deflection and rotation, shear energy due to shear strain (i.e., the difference between rotation and gradient of deflection) leads to the so-called numerical shear locking phenomena in standard finite element methods. Traditionally, shear locking has been avoided by introducing reduced numerical integration for the shear term, whereas recently the problem has been overcome by reformulations based on change of variables, for both Timoshenko beams and Reissner–Mindlin plates [44, 45]. The present three-variable formulation (2), with shear strain of the form $\varphi - \theta$, should not be prone to numerical locking either.

The natural functional space for energy (2) is the set of functions $(\alpha, \theta, \varphi) \in \mathcal{V}$ where

$$\mathcal{V} := L^2(0, L) \times L^2(0, L) \times H_0^1(0, L) \tag{3}$$

where H_0^1 stands for set of functions in the Sobolev space H^1 which vanish at $s = 0$. Note that the energy takes values in $[0, +\infty]$ on this functional space as $f \circ \alpha$ may not be integrable. Of course, this will never happen for equilibrium solutions which must have a finite energy.

We suppose that the beam is submitted to a distributed dead load represented by $\mathbf{b} \in L^2((0, L), E)$ and to concentrated load and couple \mathbf{R} and M at the free extremity $s = L$, so that the total energy reads

$$\int_0^L \left\{ k_e f(\alpha(s)) + \frac{k_b}{2} (\varphi'(s))^2 + \frac{k_t}{2} (\varphi(s) - \theta(s))^2 - \mathbf{b}(s) \cdot \boldsymbol{\chi}(s) \right\} ds - \mathbf{R} \cdot \boldsymbol{\chi}(L) - M\varphi(L) \tag{4}$$

Let us introduce the vector $\mathbf{B}(s)$, which may be interpreted as the force exerted by the right side of the beam on the left side at point s , by setting

$$\mathbf{B}(s) := \mathbf{R} + \int_s^L \mathbf{b}(\sigma) d\sigma \tag{5}$$

so that $\mathbf{B}'(s) = -\mathbf{b}(s)$ and $\mathbf{B}(L) = \mathbf{R}$. As we assumed $\boldsymbol{\chi}(0) = 0$ and as, by definition $\mathbf{B}(L) = \mathbf{R}$, integrating by parts gives

$$\int_0^L \mathbf{b}(s) \cdot \boldsymbol{\chi}(s) ds + \mathbf{R} \cdot \boldsymbol{\chi}(L) = \int_0^L \mathbf{B}(s) \cdot \boldsymbol{\chi}'(s) ds.$$

Using (1), this identity reads

$$\int_0^L \mathbf{b}(s) \cdot \boldsymbol{\chi}(s) ds + \mathbf{R} \cdot \boldsymbol{\chi}(L) = \int_0^L \alpha(s) \mathbf{B}(s) \cdot \mathbf{e}(\theta(s)) ds.$$

Therefore, the total energy can be written as a function of α , θ and φ only.

Remark 1. In the following of the paper, we will assume that the distributed load is transverse and uniform ($\mathbf{b}(s) := b \mathbf{e}_2$ for some positive constant b) and that no concentrated load or couple are applied :

$$\mathbf{R} = 0, \quad M = 0 \quad \text{and} \quad \mathbf{B}(s) = B(s) \mathbf{e}_2 \quad \text{with} \quad B(s) := b(1 - s). \tag{6}$$

Remark 2. The number of parameters in the equilibrium problem can be reduced by adimensionalizing the problem, i.e., by choosing L to be the physical length unit and by choosing the unit of energy such that $k_b = 1$. Hence, in the sequel, we fix $L = 1$ and $k_b = 1$.

2.2. Euler–Lagrange equations

The equilibrium states correspond to stationary points in \mathcal{V} of energy (4). The first variation with respect to φ , α and θ leads to the following boundary value problem¹:

$$\begin{cases} -\varphi'' + k_t(\varphi - \theta) = 0 \\ k_e g(\alpha) - \mathbf{B} \cdot \mathbf{e}(\theta) = 0 \\ k_t(\varphi - \theta) + \alpha \mathbf{B} \cdot \mathbf{e}_\perp(\theta) = 0 \\ \varphi'(1) = 0 \\ \varphi(0) = 0 \end{cases} \quad (7)$$

Remark 3. In the great majority of the textbooks of structural mechanics, the search of stationary points of (4) is performed by directly looking for the solutions of the differential problem (7), assumed as fundamental, without introducing the variational principle (4). The description of contact actions for a Timoshenko beam becomes necessary in this formulation, while starting from a variational principle this delicate issue can be skipped.

Finally, we can add that the variational formulation has several computational advantages (see for instance [46] for a general discussion and [47] for applications to beam problems).

2.3. Particular case of inextensible Euler beam

In the case $k_e = k_t = +\infty$, we have $\alpha = 1$ and $\varphi(s) = \theta(s)$ for all s . The equilibrium problem, in a nondimensional form, then reduces to the minimization of

$$\mathcal{E}(\theta) = \int_0^1 \left\{ \frac{1}{2}(\theta'(s))^2 - b(1-s) \sin(\theta(s)) \right\} ds \quad (8)$$

which corresponds to the case of a clamped inextensible Euler beam in large deformations when submitted to a uniformly distributed transverse force field (see, e.g., [48]). The first variation of (8) with respect to θ gives the boundary value problem:

$$\theta''(s) + b(1-s) \cos(\theta(s)) = 0, \quad \theta(0) = 0, \quad \theta'(1) = 0. \quad (9)$$

This boundary value problem will be studied first numerically in Sect. 3 and then analytically in Sect. 4.

3. Equilibrium configurations of Euler and Timoshenko beams: some numerical results

We focus here on problem (7) and we numerically solve it. Instead of considering problem (7) directly, we remark that, as the function g is the derivative of the convex potential f , it is a bijective function from $]0, +\infty[$ onto \mathbb{R} . Hence, from the second equation, we can write α as a function of θ . From the third equation, we can also easily write φ in terms of θ . The first equation becomes a second-order differential equation for θ . As there generally exist more than one value of $\theta(0)$ which ensures $\varphi(0) = 0$ we select the smallest one in absolute value a . It remains to satisfy the condition $\varphi'(1) = 0$. We do this by means of a

¹We introduce here the transverse unit vector $\mathbf{e}_\perp(\theta) := -\sin(\theta)\mathbf{e}_1 + \cos(\theta)\mathbf{e}_2$.

shooting technique : we replace this last condition by $\theta'(0) = k$, numerically solve the resulting Cauchy problem

$$\begin{cases} k_e g(\alpha) - \mathbf{B} \cdot \mathbf{e}(\theta) = 0 \\ k_t (\varphi - \theta) + \alpha \mathbf{B} \cdot \mathbf{e}_\perp(\theta) = 0 \\ -\varphi'' + k_t (\varphi - \theta) = 0 \\ \theta(0) = a \\ \theta'(0) = k \end{cases} \tag{10}$$

by a standard explicit Euler method for different values of the parameter k and finally select the solutions which satisfy (with prescribed accuracy) $\varphi'(1) = 0$.

Note that, in the particular case of an inextensible Euler beam model with uniformly distributed load, this parametric Cauchy problem reduces to:

$$\mathcal{P}_k = \begin{cases} \theta'' = -b(1-s)\cos\theta \\ \theta(0) = 0 \\ \theta'(0) = k. \end{cases} \tag{11}$$

In the sequel, we indicate with $\theta_k(s)$ the solution of (10) or (11). In Fig. 1, we represent $c(k) := (\theta_k)'|_{s=1}$ as a function of the parameter k . The cases $b = 30$ and $b = 60$ are represented. In Fig. 2, we show the same for $b = 200$ and $b = 1000$. It is clear that the values of k such that θ_k is a solution of (9) are, in the case of the inextensible Euler beam, the zeros of the function $c(k)$. We found them numerically with a standard application of the bisection method. These graphs suggest that the number of solutions grows as b increases. Moreover, they suggest that these solutions belong to a neighborhood of the origin depending on b . Indeed, we have:

$$c(k) = (\theta_k)'|_{s=1} = (\theta_k)'|_{s=0} + \int_0^1 \theta_k''(t) dt = k - \int_0^1 b(1-t)\cos(\theta_k(t)) dt. \tag{12}$$

Hence $|c(k) - k| \leq b$, which implies that the zeroes of the function c must belong to $[-b, b]$ and that

$$\lim_{k \rightarrow \infty} \frac{c(k)}{k} = 1 \tag{13}$$

This explains why the graph in Figs. 1 and 2 tends to a straight line with slope 1 as k diverges. Remarkably, this happens independently of the value of b .

Let us now consider the deformed shapes of the beam corresponding to equilibrium configurations. We start by showing a solution of the boundary value problem (9) (with $b = 600$) displaying a complex behavior, with three monotonicity intervals for the variable θ . As it is possible to see from Fig. 3, the angle θ never reaches the values $\frac{\pi}{2}$ or $-\frac{3\pi}{2}$ (in the last part it comes quite close to the first value). This is consistent with Proposition 1 of the following section.

In Fig. 4, we show the deformed shapes corresponding to the three solutions relative to the right panel of Fig. 1 for an inextensible Euler beam, while in Fig. 5 we show analogous equilibrium solutions for an inextensible Timoshenko beam. A comparison between the two, under the same adimensional load $b = 60$, shows² that the second model presents an overall decrease in stiffness as expected due to the presence of shear deformation; in the presented simulations the shear stiffness is set at $k_t = 7 \times 10^3$.

²It has to be remarked that another parameter enters the problem for the Timoshenko model, i.e., shear stiffness.

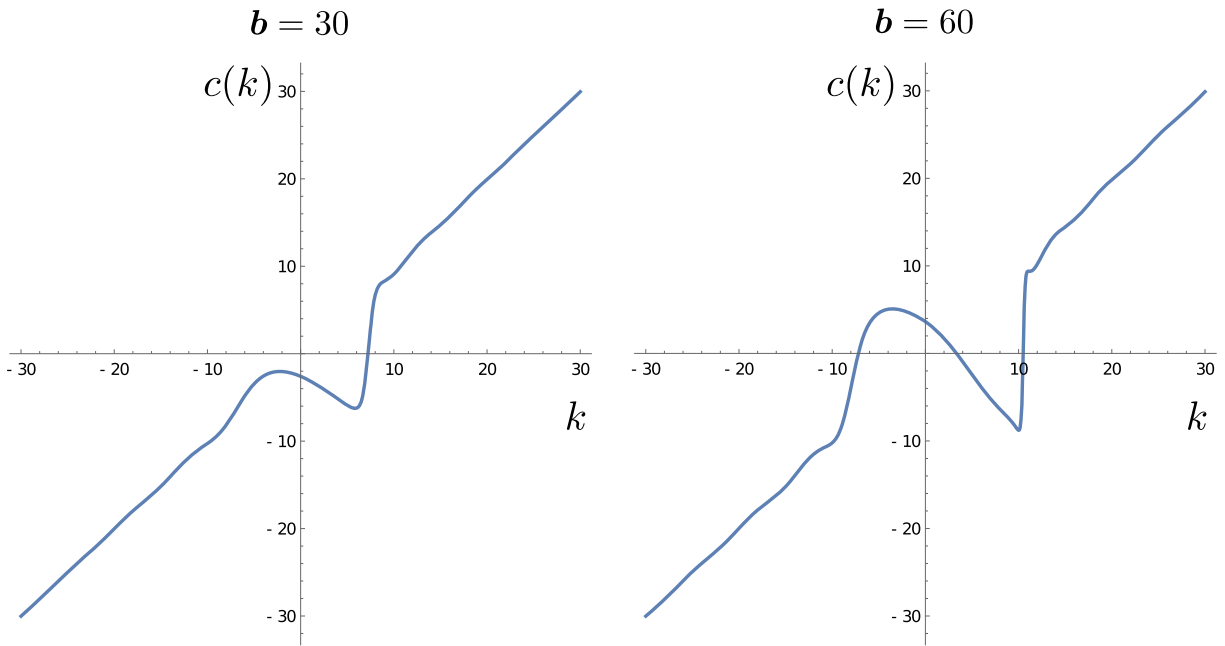


FIG. 1. Parametric shooting: $c(k)$ is plotted for two different values of the adimensional distributed load in the case of an inextensible Euler beam. The plots provide numerical evidence that the boundary value problem (9) admits one solution for $b = 30$ and three solutions for $b = 60$

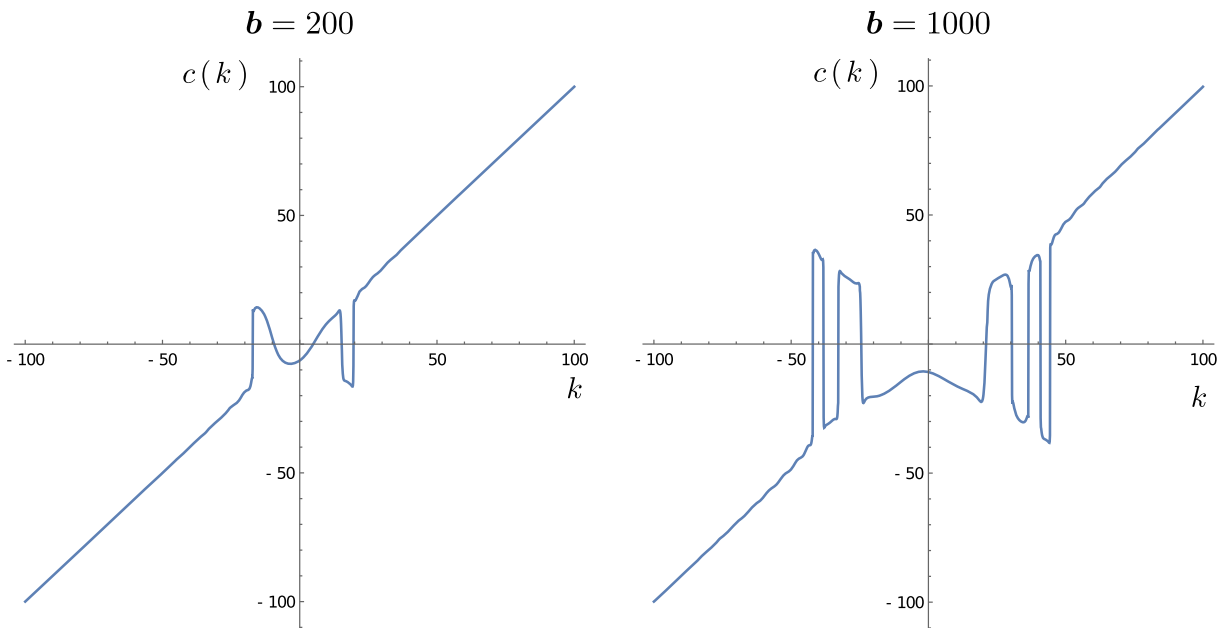


FIG. 2. Parametric shooting: $c(k)$ is plotted for two different values of the adimensional distributed load in the case of an inextensible Euler beam. The plots provide numerical evidence that the boundary value problem (9) admits five solutions for $b = 200$ and nine solutions for $b = 1000$

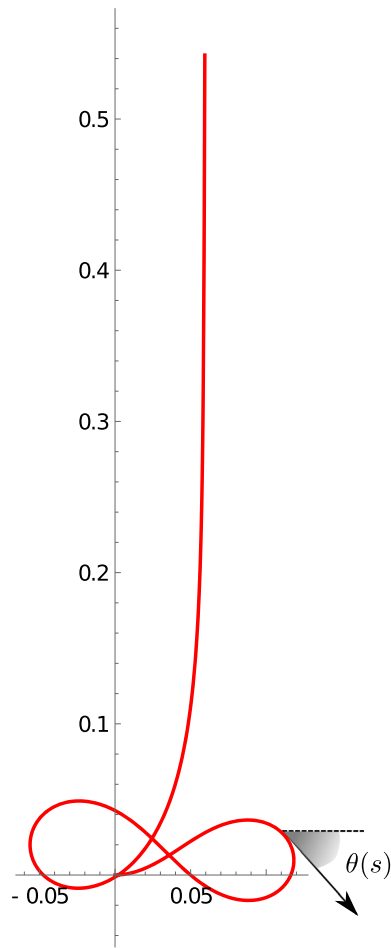


FIG. 3. A solution of the boundary value problem (9) with $b = 600$. The solution is consistent with Proposition 1. Indeed, it is possible to see that the angle θ never reaches the values $\frac{\pi}{2}$ or $-\frac{3\pi}{2}$ (in the last part it comes quite close to the first value)

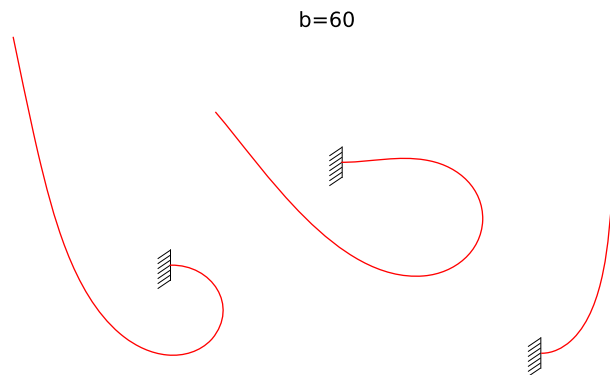


FIG. 4. Deformed shapes corresponding to the three solutions of the boundary value problem (9) with $b = 60$

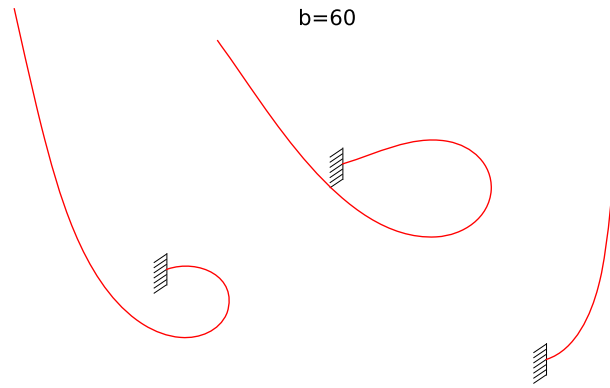


FIG. 5. The three solutions of the boundary value problem (7) with $k_e = +\infty$, $M = 0$ and $k_t = 7 \times 10^3$

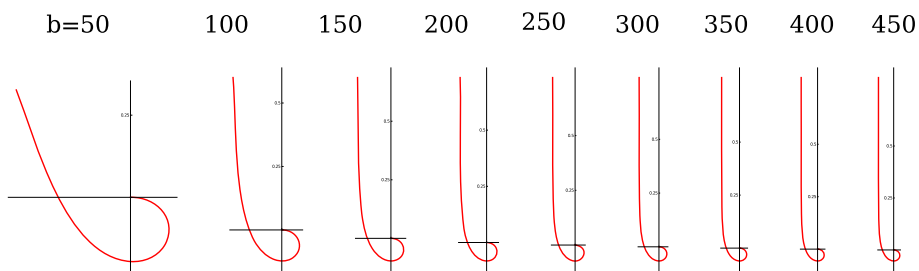


FIG. 6. Parametric study along a branch of solutions for an inextensible Euler beam model varying the transversal load b . The values of the load are indicated in the figure

Now we perform parametric studies which show the influence of the applied load b for the models considered in the paper. Four models are considered, the parameters of which are summarized in the following table. Recalling that $k_b = 1$ we consider:

	Euler inextensible Fig. 6	Euler extensible Fig. 7	Timoshenko inextensible Fig. 9	Timoshenko extensible Fig. 10
k_t	∞	∞	1.8×10^3	1.8×10^3
k_e	∞	5×10^4	∞	2×10^3

In Fig. 6, we show a set of deformed shapes of an inextensible Euler beam. The deformed shapes all belong to a branch of solutions turning around the clamped edge (see the following section for a precise definition of branches). We start from $b = 50$ and gradually increase the load up to $b = 450$.

In Fig. 7, we show a set of deformed shapes of an extensible Euler beam starting from $b = 50$, and gradually increasing the load up to $b = 450$. In this case, another parameter enters the description of the problem, i.e., the extensional stiffness k_e . We recall that the function f describing how the energy density depends on α assumed for all the simulations involving extensibility is $f = -0.01 \log(\alpha) + (\alpha - 1)^2$.

In Fig. 8, we show the plot of the functions θ and α relative to the last simulation presented in Fig. 7. In particular, it is emphasized in the figure that α attains its minimum (corresponding to the maximal local compression) in the point \bar{s} that verify $\theta(\bar{s}) = -\pi/2$, and $\alpha = 1$ in the point \bar{s} such that $\theta(\bar{s}) = -\pi$.

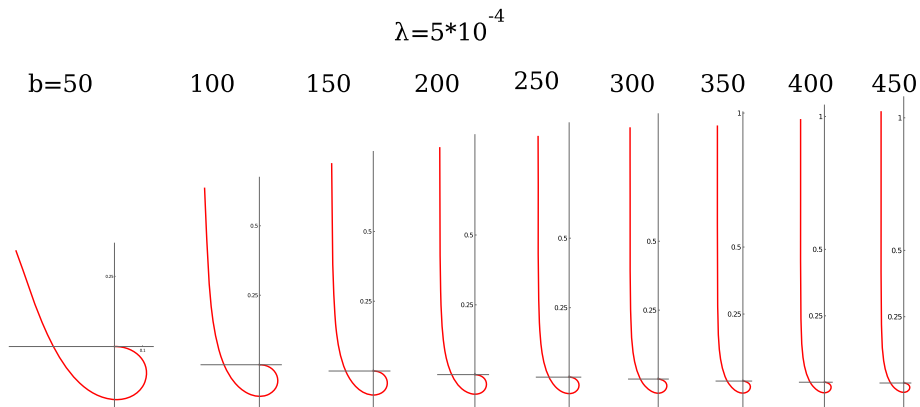


FIG. 7. Parametric study along a branch of solutions for an extensible Euler beam, varying the transversal load b . The values of the load are indicated in the figure. In these simulations, we have set $k_e = 5 \times 10^4$

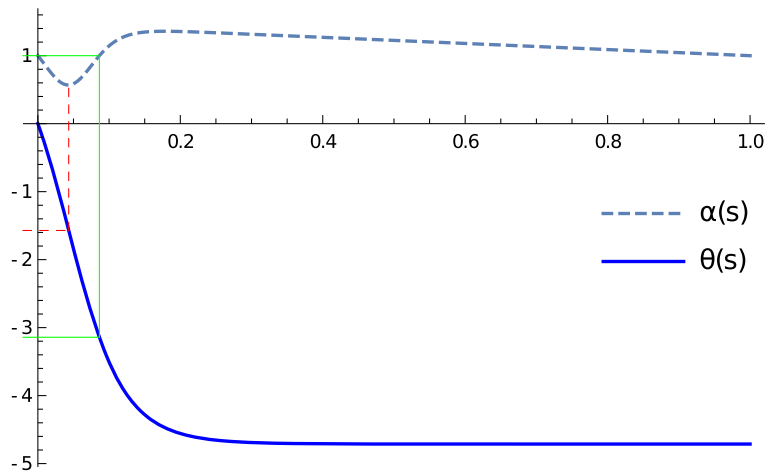


FIG. 8. θ and α for an extensible Euler beam with a transversal load $b = 450$

In Fig. 9, we show a set of deformed shapes of an inextensible Timoshenko beam starting from $b = 50$, and gradually increasing the load up to $b = 450$. Here again, another parameter is needed for the description of the problem, i.e., k_t , the shear stiffness. In these simulations, we have set $k_t = 1.8 \times 10^3$.

In Fig. 10, we show a set of deformed shapes of an extensible Timoshenko beam starting from $b = 50$, and gradually increasing the load up to $b = 450$. In this case, the two parameters introduced above, k_e and k_t are necessary. In these simulations, we have set $k_t = 1.8 \times 10^3$ and $k_e = 2 \times 10^3$.

In Fig. 11, we show the plot of the functions θ , φ and α relative to the last simulation presented in Fig. 10. As for the extensible Euler case, it is emphasized in the figure that α is minimum at the point \bar{s} that verify $\theta(\bar{s}) = -\pi/2$, and $\alpha = 1$ at the point \tilde{s} such that $\theta(\tilde{s}) = -\pi$.

Summarizing our results, we have numerical evidence that there exists a family of “curled” equilibrium configurations, that is configurations in which $|\theta(s)|$ becomes larger than π for some s . It has to be pointed out that the configurations are shown in Figs. 6, 7, 9 and 10 can be also found by a numerical minimization procedure applied to a discretized beam of the type presented in the numerical section of [49]. This suggests the conjecture that the minimizers of the energy (i.e., stable equilibria) are characterized

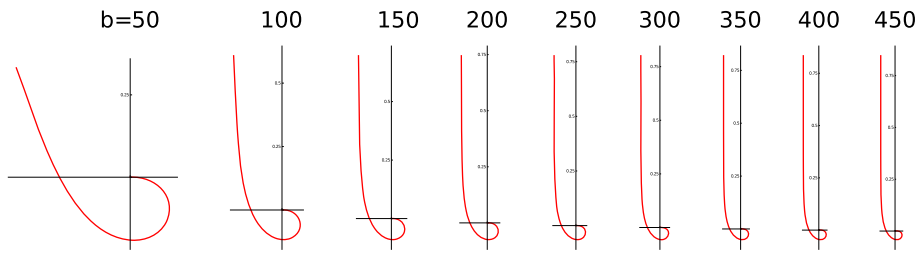


FIG. 9. Parametric study along a branch of solutions for an inextensible Timoshenko beam model varying the transversal load b . The values of the load are indicated in the figure

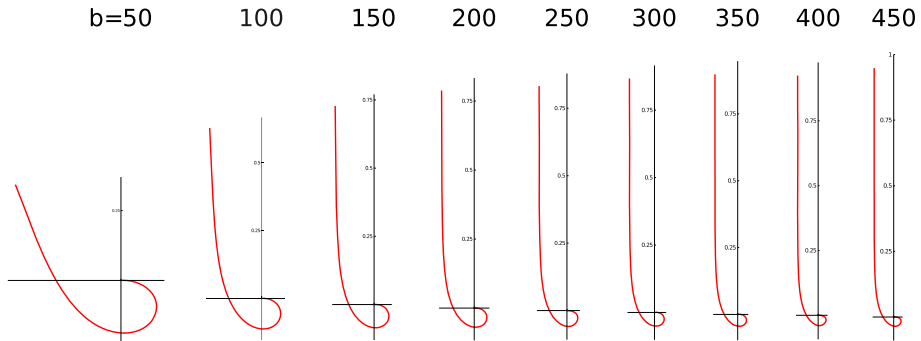


FIG. 10. Parametric study along a branch of solutions for an extensible Timoshenko beam model varying the transversal load b . The values of the load are indicated in the figure

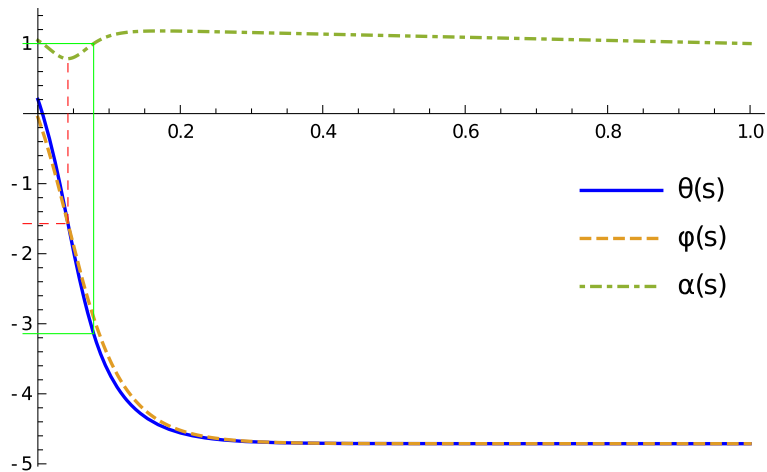


FIG. 11. θ , α and φ for an extensible Timoshenko beam with a transversal load $b = 450$

by the fact that $\theta \leq 0$ everywhere (and never reaches $\theta = -3\pi/2$). In the following section, we formalize and prove these results in the case of an inextensible Euler beam. We extend the results of [17] showing that there can exist only two branches of stable equilibrium configurations.

4. Inextensible Euler beam under distributed load: analytical results

In this section, we prove what we have seen in the numerical simulations shown in Sect. 3, i.e., that there exist a family of curled stable equilibrium configurations for the *Elastica* under distributed load. Our starting point will be the boundary value problem (9).

We classify the different types of solutions by the number of zeros of the function $\sin(\theta)$ on the interval $[0, 1]$. We say that a solution belongs to branch n of the set of equilibrium solutions if there are exactly n distinct values $0 = s_1 < s_2 < \dots < s_n$ satisfying $\sin(\theta(s_i)) = 0$.

4.1. A priori bound for the range of stationary points

Here, we prove that, for any stationary point of the functional (8), we have $-\frac{3}{2}\pi < \theta < \frac{\pi}{2}$. This means, informally speaking, that the beam cannot make a complete turn around the clamped point at the equilibrium (see Fig.12). More precisely, we establish the following:

Proposition 1. *If θ is a solution of (9), then $\sin(\theta(s)) \neq 1$ for every $s \in [0, 1]$.*

Proof. Let us define the function:

$$V(s) := \frac{1}{2}(\theta'(s))^2 + b(1-s)\sin\theta(s) - b(1-s)$$

A direct computation gives

$$V'(s) = \theta'(s)[\theta''(s) + b(1-s)\cos\theta(s)] + b(1-\sin\theta(s))$$

and, using (9),

$$V'(s) = b(1-\sin\theta(s)) \geq 0.$$

Thus V is nondecreasing and, as $V(1) = 0$, V is nonpositive in $[0, 1]$. Assume by contradiction that there exists $\bar{s} \in (0, 1) : \sin(\theta(\bar{s})) = 1$. Then $V(\bar{s}) = \frac{1}{2}(\theta'(\bar{s}))^2 \leq 0$ and thus $\theta'(\bar{s}) = 0$.

The constant function $\theta = \theta_0$ is clearly solution of the Cauchy problem made by Eq. (9) with data $\theta(\bar{s}) = \theta_0$ with $\sin(\theta_0) = 1$ and $\theta'(\bar{s}) = 0$. Uniqueness stated by Cauchy–Lipschitz theorem proves that no such a solution can satisfy $\theta(0) = 0$. \square

A graphical representation of a deformed shape that is prohibited as an equilibrium configuration for the clamped *Elastica* under uniform distributed load is shown in Fig. 12.

Remark 4. The function $V(s)$ allows us to give an estimate of the curvature at $s = 0$. Indeed, from $V(0) = \frac{1}{2}(\theta'(0))^2 - b \leq 0$, we get $|\theta'(0)| \leq \sqrt{2b}$.

Remark 5. The previous reasoning holds true as well if we replace $b(1-s)$ with any C^1 , positive and decreasing function, which corresponds to a density of force which has always the same verse (i.e., it is pointing always “upwards” or always “downwards”).

4.2. Study of equilibrium configurations for an inextensible Euler beam

In the following, we will set $B(s) := b(1-s)$. As $\sin(\theta)$ is a continuous function which does not reach 1 when θ takes values in $(-\frac{3\pi}{2}, \frac{\pi}{2})$, $\theta(s_i)$ is either 0 or $-\pi$. On an interval $[s_i, s_{i+1}]$ four situations can arise:

- **S1:** $\theta(s_i) = 0$ and $\theta'(s_i) > 0$: then θ is positive on the considered interval and $\theta(s_{i+1}) = 0$. Owing to (9), we know that θ is strictly concave, it reaches a local maximum at some unique $t_i \in (s_i, s_{i+1})$ and $\theta'(s_{i+1}) < 0$.

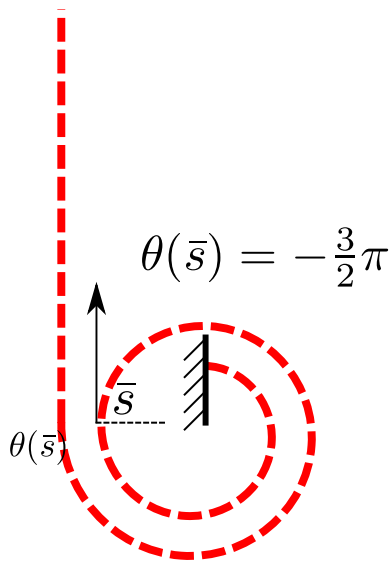


FIG. 12. Example of an “impossible” equilibrium shape for an Euler beam under distributed load: Proposition 1 proves that such a deformed shape, in which the beams turns two times around the clamp, cannot be an equilibrium configuration

- **S2:** $\theta(s_i) = 0$ and $\theta'(s_i) \leq 0$: by integrating (9) we get

$$\frac{(\theta'(s))^2}{2} = \frac{(\theta'(s_i))^2}{2} - B(s) \sin(\theta(s)) - \int_{s_i}^s B'(t) \sin(\theta(t)) dt$$

and thus $(\theta'(s))^2 > (\theta'(s_i))^2$ for $s \in (s_i, s_{i+1}]$. Therefore, θ' cannot vanish, θ is strictly decreasing, $\theta(s_{i+1}) = -\pi$ and $\theta'(s_{i+1}) < 0$.

- **S3:** $\theta(s_i) = -\pi$ and $\theta'(s_i) \leq 0$: then θ belongs to $(-\frac{3\pi}{2}, -\pi)$ on the considered interval and $\theta(s_{i+1}) = -\pi$. Owing to (9), we know that θ is strictly convex, it reaches a local minimum at some unique $t_i \in (s_i, s_{i+1})$ and $\theta'(s_{i+1}) > 0$.
- **S4:** $\theta(s_i) = -\pi$ and $\theta'(s_i) > 0$: For the same reason as in situation (S2), θ' cannot vanish, θ is strictly increasing, $\theta(s_{i+1}) = 0$ and $\theta'(s_{i+1}) > 0$.

On the interval $[s_n, 1]$, only two situations can arise which allow for θ' to vanish.

- **S1':** $\theta(s_n) = 0$ and $\theta'(s_n) > 0$: then θ is positive and strictly concave on the considered interval. It reaches its maximum at $s = 1$ where $\theta'(1) = 0$.
- **S3':** $\theta(s_n) = -\pi$ and $\theta'(s_n) \leq 0$: then θ belongs to $(-\frac{3\pi}{2}, -\pi)$, is strictly concave on the considered interval and reaches its minimum at $s = 1$ where $\theta'(1) = 0$.

Therefore, an equilibrium solution in branch n is made by a sequence of intervals in the order $S1 - S2 - S3 - S4 - S1 \dots$ ending with $S1'$ or $S3'$ and starting, if it is made by more than one interval, with $S1$ or $S2$. For instance, branches 1, 2 and 3 have, respectively, the structure $S1'$, $S2 - S3'$ and $S1 - S2 - S3'$. In general, critical points of a functional do not correspond to local minima: In that case, they correspond to unstable equilibrium solutions. To check if a solution is unstable one usually checks, if it is *linearly unstable* by computing the second Gateaux differential of the functional (8):

$$\int_0^1 [(h'(s))^2 + 2b(1-s) \sin(\theta(s))(h(s))^2] ds \tag{14}$$

The fact that this quadratic form is nonnegative is a necessary condition for stability. Actually, in the particular case of our functional, the fact that this bilinear form is positive is a sufficient condition for stability. Indeed, we have:

Lemma 1. *Let θ be a critical point of (8). If there exists a constant $C > 0$ such that, for every $h \in H^1$ verifying $h(0) = 0$,*

$$\int_0^1 \left[\frac{(h'(s))^2}{2} + b(1-s) \sin(\theta(s)) \frac{(h(s))^2}{2} \right] ds \geq C \|h\|_{H^1}^2 \quad (15)$$

then θ is a local minimizer of \mathcal{E} (defined by (8)) for the H^1 topology and therefore for the uniform norm too.

Proof. A direct computation gives

$$\begin{aligned} \mathcal{E}(\theta + h) &= \mathcal{E}(\theta) + \int_0^1 [\theta' h' - B \cos(\theta) h] ds \\ &+ \int_0^1 \left[\frac{(h')^2}{2} + B \sin(\theta) \frac{h^2}{2} - B \left(\sin(\theta) (\cos(h) - 1 + \frac{h^2}{2}) + \cos(\theta) (\sin(h) - h) \right) \right] ds \end{aligned}$$

Integrating by parts, the second addend can be rewritten

$$\int_0^1 [\theta' h' - B \cos(\theta) h] ds = \theta'(1)h(1) - \theta'(0)h(0) - \int_0^1 [\theta''(s) - B \cos(\theta(s))] h(s) ds$$

Let θ be a critical point for \mathcal{E} . It satisfies (9) and, as $h(0) = 0$, all terms in the above sum vanish. Using moreover inequality (15), we get the estimation

$$\begin{aligned} &\mathcal{E}(\theta + h) - \mathcal{E}(\theta) - C \|h\|_{H^1}^2 \\ &\geq - \int_0^1 B \left(\sin(\theta) (\cos(h) - 1 + \frac{h^2}{2}) + \cos(\theta) (\sin(h) - h) \right) ds \\ &\geq -b \int_0^1 \left[\left| \cos(h) - 1 + \frac{h^2}{2} \right| + |\sin(h) - h| \right] ds \end{aligned}$$

Let η be such that $0 < \eta < \frac{C}{2b}$. There exists $\epsilon > 0$ such that $0 < x < \epsilon$ implies $|\cos(x) - 1 + \frac{x^2}{2}| < \eta x^2$ and $|\sin(x) - x| < \eta x^2$. Hence, for every h such that $\|h\|_{H^1} < \epsilon$, which implies $\|h\|_{L^\infty} < \epsilon$, we have:

$$\int_0^1 \left[\left| \cos(h) - 1 + \frac{h^2}{2} \right| + |\sin(h) - h| \right] ds < 2\eta \int_0^1 h^2 < 2\eta \|h\|_{H^1}^2.$$

Therefore, we obtain that, for any h with $\|h\|_{H^1} < \epsilon$,

$$\mathcal{E}(\theta + h) - \mathcal{E}(\theta) \geq (C - 2b\eta) \|h\|_{H^1}^2$$

□

In the following propositions, we will completely characterize the stable equilibrium configurations of the *Elastica* under distributed load. Indeed, we show that branch 1 corresponds to global minimizers of the functionals and thus to stable equilibrium solutions, that branch 2 corresponds, for b large enough, to other stable equilibrium solutions while all other branches are unstable.

Proposition 2. *For any b , there exists a unique corresponding solution in branch 1. This solution is the global minimizer of the functional (8).*

Proof. The existence of a global minimizer θ of the functional (8) is assured by the coercivity and lower semi-continuity of the functional. The function $\tilde{\theta} := -\frac{\pi}{2} + \left| \frac{\pi}{2} + \theta \right|$ has the same energy as θ and takes values in $(-\frac{\pi}{2}, \frac{\pi}{2})$. The truncated function $\bar{\theta} := \max(0, \tilde{\theta})$ (which clearly is in H_0^1) has a lower energy (strictly lower if θ does not belong to branch 1) and takes values in $[0, \frac{\pi}{2})$. Hence, any global minimizer takes values in $(0, \frac{\pi}{2})$: It must belong to branch 1. Let us now prove that, for a given b , there exists at most one solution in branch 1. By contradiction, let us consider two distinct solutions θ_1 and θ_2 . We have $\theta_1'(0) \neq \theta_2'(0)$ owing to Cauchy–Lipschitz uniqueness property. We can therefore suppose that $\theta_1'(0) < \theta_2'(0)$. We then introduce $s_1 > 0$ as the maximum value such that $\theta_1 < \theta_2$ on the interval $(0, s_1)$. On $(0, s_1)$ we have $\cos(\theta_1) > \cos(\theta_2)$, thus $-B \cos(\theta_1) < -B \cos(\theta_2)$, $\theta_1' < \theta_2'$ and so $\theta_1' < \theta_2'$. As a consequence $\theta_1(s_1) < \theta_2(s_1)$ which is in contradiction with the definition of s_1 and the continuity of functions θ_1 and θ_2 unless $s_1 = 1$. But in that case $\theta_1'' < \theta_2''$ implies also $\theta_1'(1) < \theta_2'(1)$ which is in contradiction with the fact that $\theta_1'(1) = \theta_2'(1) = 0$. \square

To prove that any solution θ in branch n for $n > 2$ is unstable, let us remark that it must contain an interval of type S1 or S3. Hence, there are at least two distinct points t_i, t_j such that $\theta'(t_i) = \theta'(t_j) = 0$. This prevents linear stability. Indeed, we have:

Proposition 3. *Any solution containing a part defined over $[s_1, s_2] \subset [0, 1]$ such that $\theta'(s_1) = \theta'(s_2) = 0$ is unstable. Thus only branches 1 and 2 can be stable.*

Proof. Let us check the second variation

$$V := \int_0^1 \left[\frac{(h'(s))^2}{2} + b(1-s) \sin(\theta(s)) \frac{(h(s))^2}{2} \right] ds$$

with $h = \theta' 1_{[s_1, s_2]}$ (here by 1_X we denote the characteristic function of the set X). We have:

$$V = \int_{s_1}^{s_2} \left[\frac{(\theta''(s))^2}{2} + \frac{1}{2} (b(1-s)\theta'(s))(\sin(\theta(s))\theta'(s)) \right] ds$$

and after integrating by parts the second term:

$$V = \int_{s_1}^{s_2} \left[\frac{(\theta''(s))^2}{2} + \frac{1}{2} (b(1-s)\theta''(s) - b\theta'(s)) \cos(\theta(s)) \right] ds$$

Recalling Eq. (7), we have:

$$\begin{aligned} V &= - \int_{s_1}^{s_2} \left[\frac{1}{2} b\theta'(s) \cos(\theta(s)) \right] ds \\ &= - \int_{s_1}^{s_2} \left[\frac{1}{2} \frac{b(1-s)}{1-s} \theta'(s) \cos(\theta(s)) \right] ds \end{aligned}$$

Recalling again Eq. (7) and integrating by parts once more:

$$\begin{aligned} V &= + \int_{s_1}^{s_2} \left[\frac{1}{2} \frac{\theta''(s)\theta'(s)}{1-s} \right] ds \\ &= - \int_{s_1}^{s_2} \left[\frac{1}{4} \frac{(\theta'(s))^2}{(1-s)^2} \right] ds < 0 \end{aligned}$$

□

It remains to study branch 2. We prove that, for b large enough, the energy possesses some local minimizers which belong to branch 2 and therefore are stable solutions.

Proposition 4. *For b large enough, branch 2 contains stable solutions.*

Proof. We first remark that the energy minimization problem

$$\min_{\theta} \int_0^1 \left(\frac{(\theta'(s))^2}{2} + b(1-s)(1 - \sin(\theta(s))) \right) ds$$

can be rewritten, by setting $u = \frac{\pi}{4} + \frac{\theta}{2}$ and rescaling, as $\min_{u \in \mathcal{S}} F(u)$ where

$$F(u) := \int_0^1 ((u'(s))^2 + 2b(1-s)\cos^2(u(s))) ds$$

and the set \mathcal{S} of admissible u is now the set of functions in $H^1(0, 1)$ taking values in $(-\frac{\pi}{2}, \frac{\pi}{2})$ and satisfying $u(0) = \frac{\pi}{4}$.

Let us assume $b^{1/4} > 100$ (which is not an optimal value) and denote $\delta := b^{-1/4}$. Consider the set \mathcal{O} of functions u in \mathcal{S} satisfying $u(\delta) < 0$ and its closure $\bar{\mathcal{O}}$, i.e., the set of functions u in \mathcal{S} satisfying $u(\delta) \leq 0$. We will prove that there exists a local minimizer of the energy in \mathcal{O} . Such a local minimizer cannot correspond to a critical solution in branch $n > 2$ as we already know that such a solution is unstable. Neither it can belong to branch 1 as $u(\delta) \leq 0$. Therefore, it must belong to branch 2. To prove that there exists a local minimizer of the energy in \mathcal{O} , we consider a minimizer \bar{u} of the energy in $\bar{\mathcal{O}}$ (its existence is clearly ensured as $\bar{\mathcal{O}}$ is closed with respect to the H^1 topology) and check that it actually belongs to \mathcal{O} .

We first establish an upperbound for $F(\bar{u})$. Setting $s_0 := \frac{\ln(\sqrt{2}+1)}{\sqrt{b}}$, the function v defined by $v(s) := \frac{\pi}{2} - 2 \arctan(e^{\sqrt{b}(s-s_0)})$ belongs to $\bar{\mathcal{O}}$. Indeed, $v(s) < 0$ as soon as $s > s_0$ and this is the case for $s = \delta$. Moreover, noticing that $v' = -\sqrt{b}\cos(v)$, we can upperbound $F(v)$ by

$$F(v) \leq \int_0^1 ((v'(s))^2 + b\cos^2(v(s))) ds = -2 \int_0^1 \left(\sqrt{b}\cos(v(s))v'(s) \right) ds \leq 4\sqrt{b}.$$

Therefore $F(\bar{u}) \leq F(v) \leq 4\sqrt{b}$.

Let us now assume, by contradiction, that $\bar{u} \notin \mathcal{O}$. This means $\bar{u}(\delta) = 0$. Using previous estimation, we get

$$\int_0^{\delta} b(1-\delta)\cos^2(\bar{u}(s)) ds \leq \int_0^{\delta} b(1-s)\cos^2(\bar{u}(s)) ds \leq 4\sqrt{b}.$$

Thus, there exists some $t_1 \in (0, \delta)$ such that

$$\cos^2(\bar{u}(t_1)) \leq \frac{4\sqrt{b}}{b(1-\delta)\delta} \leq \frac{4}{99}.$$

and $|\sin(\bar{u}(t_1))| \geq \sqrt{\frac{95}{99}} \geq \frac{95}{99}$. For a similar reason, there exists some $t_2 \in (\delta, 2\delta)$ such that $|\sin(\bar{u}(t_2))| \geq \frac{94}{98}$. We can estimate $F(\bar{u})$ on the different intervals $[0, t_1]$, $[t_1, \delta]$, $[\delta, t_2]$. On each one, we use the estimate:

$$\begin{aligned} \int_x^y ((\bar{u}'(s))^2 + b(1-s)\cos^2(\bar{u}(s))) \, ds &\geq 2 \int_x^y ((\bar{u}'(s))^2 + b(1-y)\cos^2(\bar{u}(s))) \, ds \\ &\geq 2 \int_x^y \sqrt{b(1-y)} |\cos(\bar{u}(s))\bar{u}'(s)| \, ds \\ &\geq 2\sqrt{b(1-y)} |\sin(\bar{u}(y)) - \sin(\bar{u}(x))|. \end{aligned}$$

We obtain the contradiction :

$$\begin{aligned} F(\bar{u}) &\geq 2\sqrt{b(1-2\delta)} \left(|\sin(\bar{u}(t_1)) - \sin(\frac{\pi}{4})| + |\sin(\bar{u}(t_1))| + |\sin(\bar{u}(t_2))| \right) \\ &\geq 2 \times \frac{98}{100} \left(\frac{95}{99} - \frac{\sqrt{2}}{2} + \frac{95}{99} + \frac{94}{98} \right) \sqrt{b} \geq 4\sqrt{b}. \end{aligned}$$

which completes the proof. \square

5. Conclusion

We have classified the equilibria of nonlinear Euler and Timoshenko beams subjected to uniformly distributed load. We have identified sequences of equilibria among which two at most are stable. The methods and techniques used here are rather simple and could be efficiently generalized to attack more general theories of beams formulated in order to take into account different kinds of effects. We think of beams with deformation of the section or differentiated deformations of different layers in composite beams [50], strain concentration in thin-walled beams, piezoelectric activated deformations [51].

Another possible extension of the presented result could be the study of the problem introduced in [52] of equilibria of beams constrained to remain on a given smooth surface.

Publisher's Note Springer Nature remains neutral with regard to jurisdictional claims in published maps and institutional affiliations.

References

- [1] Euler, L., Carathéodory, C.: *Methodus Inveniendi Lineas Curvas Maximi Minimive Proprietate Gaudentes Sive Solutio Problematis Isoperimetrici Latissimo Sensu Accepti*, vol. 1. Springer, Berlin (1952)
- [2] Bernoulli, D.: The 26th letter to Euler. *Corresp. Math. Phys.* **2**, 1742 (1843)
- [3] Bernoulli, J.: *Quadratura curvae, e cujus evolutione describitur inflexae laminae curvatura*. *Die Werke von Jakob Bernoulli* **1691**, 223–227 (1692)
- [4] Antman, S.S., Renardy, M.: Nonlinear problems of elasticity. *SIAM Rev.* **37**(4), 637 (1995)
- [5] Steigmann, D.J.: *Finite Elasticity Theory*. Oxford University Press, Oxford (2017)
- [6] Bisshopp, K.E., Drucker, D.C.: Large deflection of cantilever beams. *Q. Appl. Math.* **3**(3), 272–275 (1945)
- [7] Fertis, D.G.: *Nonlinear Structural Engineering*. Springer, Berlin (2006)
- [8] Ladevèze, P.: *Nonlinear Computational Structural Mechanics: New Approaches and Non-incremental Methods of Calculation*. Springer, Berlin (2012)

- [9] Steigmann, D.J.: Invariants of the stretch tensors and their application to finite elasticity theory. *Math. Mech. Solids* **7**(4), 393–404 (2002)
- [10] Nizette, M., Goriely, A.: Towards a classification of Euler–Kirchhoff filaments. *J. Math. Phys.* **40**(6), 2830–2866 (1999)
- [11] Goriely, A., Nizette, M., Tabor, M.: On the dynamics of elastic strips. *J. Nonlinear Sci.* **11**(1), 3–45 (2001)
- [12] Hamdouni, A., Millet, O.: An asymptotic non-linear model for thin-walled rods with strongly curved open cross-section. *Int. J. Non Linear Mech.* **41**(3), 396–416 (2006)
- [13] Luongo, A., Zulli, D.: *Mathematical Models of Beams and Cables*. Wiley, New York (2013)
- [14] Piccardo, G., D’Annibale, F., Luongo, A.: A perturbation approach to the nonlinear generalized beam theory. In: 4th Canadian Conference on Nonlinear Solid Mechanics (CanCNSM 2013) (2013)
- [15] Taig, G., Ranzi, G., D’annibale, F.: An unconstrained dynamic approach for the generalised beam theory. *Contin. Mech. Thermodyn.* **27**(4–5), 879 (2015)
- [16] Piccardo, G., Ranzi, G., Luongo, A.: A complete dynamic approach to the generalized beam theory cross-section analysis including extension and shear modes. *Math. Mech. Solids* **19**(8), 900–924 (2014)
- [17] Della Corte, A., dell’Isola, F., Esposito, R., Pulvirenti, M.: Equilibria of a clamped euler beam (elastica) with distributed load: large deformations. *Mathem. Models Methods Appl. Sci.* **27**, 1–31 (2016)
- [18] dell’Isola, F., Giorgio, I., Pawlikowski, M., Rizzi, N.L.: Large deformations of planar extensible beams and pantographic lattices: heuristic homogenization, experimental and numerical examples of equilibrium. *Proc. R. Soc. A* **472**, 20150790 (2016)
- [19] Bungartz, H.-J., Schäfer, M.: *Fluid–Structure Interaction: Modelling, Simulation, Optimisation*, vol. 53. Springer, Berlin (2006)
- [20] Bazilevs, Y., Takizawa, K., Tezduyar, T.E.: *Computational Fluid–Structure Interaction: Methods and Applications*. Wiley, New York (2013)
- [21] Solaria, G., Pagnini, L.C., Piccardo, G.: A numerical algorithm for the aerodynamic identification of structures. *J. Wind Eng. Ind. Aerodyn.* **69**, 719–730 (1997)
- [22] Pagnini, L.C.: A numerical approach for the evaluation of wind-induced effects on inclined, slender structural elements. *Eur. J. Environ. Civ. Eng.* **21**, 1–20 (2016)
- [23] Liberge, E., Pomarede, M., Hamdouni, A.: Reduced-order modelling by pod-multiphase approach for fluid–structure interaction. *Eur. J. Comput. Mech. Revue Eur. Méc. Numér.* **19**(1–3), 41–52 (2010)
- [24] Pideri, C., Seppecher, P.: A second gradient material resulting from the homogenization of an heterogeneous linear elastic medium. *Contin. Mech. Thermodyn.* **9**(5), 241–257 (1997)
- [25] Forest, S., Sievert, R.: Nonlinear microstrain theories. *Int. J. Solids Struct.* **43**(24), 7224–7245 (2006)
- [26] Atai, A.A., Steigmann, D.J.: On the nonlinear mechanics of discrete networks. *Arch. Appl. Mech.* **67**(5), 303–319 (1997)
- [27] Boutin, C., Giorgio, I., Placidi, L., et al.: Linear pantographic sheets: asymptotic micro-macro models identification. *Math. Mech. Complex Syst.* **5**(2), 127–162 (2017)
- [28] Placidi, L., Andreaus, U., Giorgio, I.: Identification of two-dimensional pantographic structure via a linear d4 orthotropic second gradient elastic model. *J. Eng. Math.* **103**(1), 1–21 (2017)
- [29] Scerrato, D., Giorgio, I., Rizzi, N.L.: Three-dimensional instabilities of pantographic sheets with parabolic lattices: numerical investigations. *Z. Angew. Math. Phys.* **67**(3), 53 (2016)
- [30] Turco, E., Golaszewski, M., Cazzani, A., Rizzi, N.L.: Large deformations induced in planar pantographic sheets by loads applied on fibers: experimental validation of a discrete Lagrangian model. *Mech. Res. Commun.* **76**, 51–56 (2016)
- [31] Turco, E., Golaszewski, M., Giorgio, I., D’Annibale, F.: Pantographic lattices with non-orthogonal fibres: experiments and their numerical simulations. *Compos. Part B Eng.* **118**, 1–14 (2017)
- [32] Turco, E., Golaszewski, M., Giorgio, I., Placidi, L.: Can a Hencky-type model predict the mechanical behaviour of pantographic lattices? In: Dell’Isola, F. (ed.) *Mathematical Modelling in Solid Mechanics*, pp. 285–311. Springer, Berlin (2017)
- [33] Placidi, L., Barchiesi, E., Turco, E., Rizzi, N.L.: A review on 2d models for the description of pantographic fabrics. *Z. Angew. Math. Phys.* **67**(5), 121 (2016)
- [34] Kalpakjian, S., Vijai Sekar, K.S., Schmid, S.R.: *Manufacturing Engineering and Technology*. Pearson, London (2014)
- [35] Misra, A., Placidi, L., Scerrato, D.: A review of presentations and discussions of the workshop computational mechanics of generalized continua and applications to materials with microstructure that was held in Catania 29–31 October 2015. *Math. Mech. Solids* **9**, 1891–1904 (2016)
- [36] Nase, M., Rennert, M., Naumenko, K., Eremeyev, V.A.: Identifying tractionseparation behavior of self-adhesive polymeric films from in situ digital images under t-peeling. *J. Mech. Phys. Solids* **91**, 40–55 (2016)
- [37] Faulkner, M.G., Lipsett, A.W., Tam, V.: On the use of a segmental shooting technique for multiple solutions of planar elastica problems. *Comput. Methods Appl. Mech. Eng.* **110**(3–4), 221–236 (1993)
- [38] Raboud, D.W., Faulkner, M.G., Lipsett, A.W.: Multiple three-dimensional equilibrium solutions for cantilever beams loaded by dead tip and uniform distributed loads. *Int. J. Non Linear Mech.* **31**(3), 297–311 (1996)
- [39] Timoshenko, S.P.: Lxvi. On the correction for shear of the differential equation for transverse vibrations of prismatic bars. *Lond. Edinb. Dublin Philos. Mag. J. Sci.* **41**(245), 744–746 (1921)

- [40] Timoshenko, S.P.: X. On the transverse vibrations of bars of uniform cross-section. Lond. Edinb. Dublin Philos. Mag. J. Sci. **43**(253), 125–131 (1922)
- [41] Cosserat, E., Cosserat, F., et al.: *Théorie des corps déformables*. A. Hermann et fils, Paris (1909)
- [42] Altenbach, H., Birsan, M., Eremeyev, V.A.: Cosserat-type rods. In: Altenbach, H. (ed.) *Generalized Continua from the Theory to Engineering Applications*, pp. 179–248. Springer, Berlin (2013)
- [43] Altenbach, J., Altenbach, H., Eremeyev, V.A.: On generalized cosserat-type theories of plates and shells: a short review and bibliography. Arch. Appl. Mech. **80**(1), 73–92 (2010)
- [44] Balabanov, V., Niiranen, J.: Locking-free variational formulations and isogeometric analysis for the Timoshenko beam models of strain gradient and classical elasticity. Comput. Methods Appl. Mech. Eng. **339**, 137–159 (2018)
- [45] Beirao da Veiga, L., Hughes, T.J.R., Kiendl, J., Lovadina, C., Niiranen, J., Reali, A., Speleers, H.: A locking-free model for Reissner–Mindlin plates: analysis and isogeometric implementation via nurbs and triangular nurps. Math. Models Methods Appl. Sci. **25**, 1519–1551 (2015)
- [46] Capobianco, G., Eugster, S.R.: Time finite element based Moreau-type integrators. Int. J. Numer. Methods Eng. **114**(3), 215–231 (2018)
- [47] Eugster, S.R., Hesch, C., Betsch, P., Glocker, C.: Director-based beam finite elements relying on the geometrically exact beam theory formulated in skew coordinates. Int. J. Numer. Methods Eng. **97**(2), 111–129 (2014)
- [48] Eugster, S.R., et al.: *Geometric Continuum Mechanics and Induced Beam Theories*, vol. 75. Springer, Berlin (2015)
- [49] Alibert, J.-J., Della Corte, A., Giorgio, I., Battista, A.: Extensional elastica in large deformation as Γ -limit of a discrete 1D mechanical system. Z. Angew. Math. Phys. **68**(2), 42 (2017)
- [50] Birsan, M., Altenbach, H., Sadowski, T., Eremeyev, V.A., Pietras, D.: Deformation analysis of functionally graded beams by the direct approach. Compos. Part B Eng. **43**, 1315–1328 (2012)
- [51] Chróscielewski, J., Schmidt, R., Eremeyev, V.A.: Nonlinear finite element modeling of vibration control of plane rod-type structural members with integrated piezoelectric patches. Contin. Mech. Thermodyn. **31**, 1–42 (2018)
- [52] Javili, A., McBride, A., Steinmann, P.: Thermomechanics of solids with lower-dimensional energetics: on the importance of surface, interface, and curve structures at the nanoscale. a unifying review. Appl. Mech. Rev. **65**, 010802 (2013)

A. Della Corte, A. Battista, F. dell’Isola and P. Seppecher
M&MoCS, Research Center
University of L’Aquila
L’Aquila
Italy
e-mail: alessandro.dellacorte.memocs@gmail.com

A. Battista
e-mail: antoniobattista1986@gmail.com

F. dell’Isola
e-mail: fdellisola@gmail.com

P. Seppecher
e-mail: seppecher@imath.fr

A. Battista
Université de La Rochelle
La Rochelle
France

F. dell’Isola
DISG
University La Sapienza
Rome
Italy

P. Seppecher
IMATH
Université de Toulon
Toulon
France

(Received: July 26, 2018; revised: February 21, 2019)